Simultaneous measure of refractive index and thickness of dielectric plane parallel plates by fringe counting: a case for generalized regression

G. Rodriguez-Zurita[1,3], R. Pastrana-Sanchez[2], and J. Vazquez-Castillo[1]
[1] *Centro de Investigaciones en Óptica*
Apartado postal 1-948, 37000 Leon, Gto., Mexico
[2] *Facultad de Ciencias Fisico-Matemáticas, Benemérita Universidad Autónoma de Puebla*
Apartado postal 1157, 72000 Puebla, Pue., Mexico
[3] *e-mail: gzurita@fcfm.buap.mx*

Recibido el 25 de septiembre de 1998; aceptado el 10 de marzo de 1999

Measurement of refractive index and thickness of a plane parallel dielectric plate is proposed as a laboratory exercise on Physical Optics employing the technique of counting interference fringes. The plate under inspection is tilted in one of the arms of an appropiate interferometer, thereby causing the interference fringes to shift. When the fringes are adjusted to be concentric rings, the shift produces an apparent shrinkage or expanding of the rings. Counting fringes which contract or expand gives an idea of the phase changes as a function of tilting angle. Such readings can be compared with the theoretical shift, which can be found by geometric considerations. Besides, due to the mathematical form of the derived phase behaviour, the readings become an example of data to be subject of a generalized regression fitting. Because some math software packages include functions designed to do such a fitting, they can be directly used to complete the experimental data processing, thus making a quantitative comparison with the theory. The report of experimental results and discussion on several alternatives for fitting are presented. Among these, the simultaneous estimation of both refractive index and thickness are emphasized.

Keywords: Interferometers; laboratory experiments and apparatus; interference; parallelism

Se propone la medición del índice de refracción y del espesor de placas dieléctricas plano-paralelas como un ejercicio de laboratorio de óptica empleando la técnica del conteo de franjas de interferencia. La placa bajo inspección se inclina en uno de los brazos de un interferómetro, causando que las franjas de interferencia sufran un corrimiento. Ajustando las franjas para obtener anillos concéntricos, éstos sufren un encogimiento o expansión aparentes dependiendo del valor del corrimiento inducido. El conteo de anillos colapsándose o expandiéndose proporciona una idea de los cambios respectivos de fase como función del ángulo de inclinación, de modo que las lecturas pueden compararse con el corrimiento teórico, el cual puede hallarse bajo consideraciones geométricas. Además, debido a la forma matemática del comportamiento de la fase, las lecturas tomadas representan un ejemplo de datos apropiados para un ajuste de regresión generalizada. Dado que algunos paquetes de cómputo incluyen funciones diseñadas para realizar tales ajustes, pueden emplearse directamente para complementar el procesamiento de datos y realizar una comparación cuantitativa con la teoría. Se presenta el reporte de resultados experimentales y se discuten varias alternativas de ajuste. De entre éllas, se destaca la posibilidad de la simultánea medición del índice de refracción y del espesor de la placa.

Descriptores: Interferómetros; experimentos y arreglos experimentales; interferencia; paralelismo

PACS: 07.60.Ly; 01.50.Pa; 42.25.Hz

1. Introduction

Fringe counting is a classical optical interferometric technique to estimate optical path differences (for example, in multiples of some wavelength) between two interfering waves by keeping track of the number of interference fringes passing through a given reference point while changing the optical path length of one of those waves [1]. The technique is widely used in the teaching physics laboratory while working with interferometers of the Michelson or Fabry-Perot type in order to measure length differences (in wavelength units, for example) or unknown wavelengths [2]. On the other hand, inspection of parallelism of transparent plates can be carried out inserting the plate in one arm of a suitable two-beam interferometer, such as a Mach-Zehnder interferometer. With this method, it is also possible to measure the plate's refractive index if the plate thickness is known (or measured separately) [3]. Conversely, knowledge of refractive index leads to determination of thickness [3]. Constant angle interference spectroscopy has been proposed to measure refractive index and thickness of transparent layers [4]. These techniques use several wavelengths and holds the tilt angle fixed. Variable angle monochromatic fringe observation, another type of measurements, requires two or more wavelengths to determine both parameters, as reported earlier [4]. Along this communication, the fringe counting method is described as experimentally applied to a step-wise tilting dielectric plate to inspect the parallelism of its two wider planar faces. In particular, it is emphasized that the technique is also able to led to the simultaneous determination of both refractive index and thickness of the plate on the basis of the same data set, using just one wavelength, and an appropiate fitting. Because

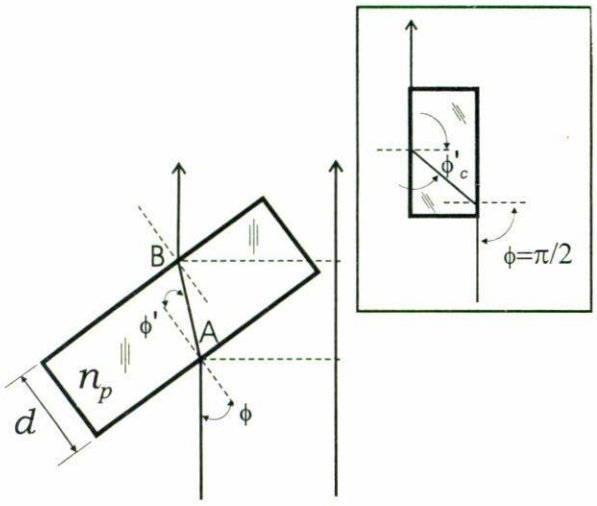

FIGURE 1. Determination of the OPD as a function of the entrance angle ϕ. ϕ' is the refracting angle, n_p the plate's refractive index, and d its thickness. Inserted figure: grazing incidence case. ϕ'_c is the critical angle.

the fringe shifts rather admit generalized regression fittings, the interferometric inspection of plates as described offers a good opportunity to employ corresponding functions included in some commercial software packages for advanced mathematical calculations. Data processing using a widely spread math package is also presented [5].

2. OPD of tilted plates

First, we consider the fringe shifts of the interference pattern between two waves, one of which pass through a tilted transparent plate.

2.1. Interference pattern shifts

Figure 1 depicts a ray impinging on a plane-parallel plate at an angle ϕ. Such a ray is deviated from its original path and cross through a new path AB. The optical path difference (OPD) with respect to a ray which do not pass through the plate can be shown to be

$$\mathrm{OPD} = dn_{\mathrm{P}}\left[1-\left(\frac{\sin\phi}{n_{\mathrm{P}}}\right)^2\right]^{-\frac{1}{2}} - dn, \qquad (1)$$

where d denotes the plate thickness, n_p the plate refractive index, and n the environment s refractive index. When a beam having crossing the plate is placed in superposition with an external reference wave, the ideal phase difference $\Phi(\phi)$ of the emerging beam is given by

$$\Phi(\phi) = \frac{2\pi d}{\lambda}\left\{n_{\mathrm{P}}\left[1-\left(\frac{\sin\phi}{n_{\mathrm{P}}}\right)^2\right]^{-\frac{1}{2}} - n\right\}, \qquad (2)$$

where λ denotes the wavelength associated to the beam. As a result of the beam superposition, the conditions outlined render an irradiance pattern $I(\vec{r},\phi)$ of the form

$$I(\vec{r},\phi) = a\cdot\{1+m\cdot\cos[\alpha(\vec{r},\phi)+\Phi(\phi)]\}, \qquad (3)$$

where it is seen that the fringe pattern has to be shifted by an amount $\Phi(\phi)$ as the entrance angle ϕ changes. In the above equation, $\alpha(\vec{r},\phi)$ denotes a given wavefront distribution on position $\vec{r}$ at the observation plane [$\alpha(\vec{r},\phi)$ includes the lateral displacement of the beam], a is the corresponding irradiance background, and m the fringe modulation.

2.2. Circular interference patterns

For the case of incident plane waves, $\alpha(\vec{r},\phi)$ carries the information of some amount of spherical aberration due to the crossing of one beam through the plate. When one of the beams are slightly adjusted out of focus, the interference fringes tend to adopt concentric ring shapes in addition to the shaping due to spherical aberration and the lateral displacement. But these two contributions can be neglected by making the observations at the centre of the circular pattern. The phase shift $\Phi(\phi)$, on the other hand, will cause the ring radius to "shrink" or to "grow". Then, the rings in the interference pattern appear to contract or to expand. In this case, fringe counting consists in keeping track of the number of rings which contract into (or emerge from) the centre of the circular pattern.

According with the previous observations, it is possible to pay attention on $\Phi(\phi)$ as the only effect responsible to the main changes of interference patterns when a plate is tilted as described. Inspection of Eq. (2), to begin with, shows that $\Phi(\phi)$ is a periodic function of period π, and with maximum and minimum values given by $\Phi_{\max} = \Phi(\pi/2)$ and $\Phi_{\min} = \Phi(0)$, respectively. Thus, the width range of values of $\Phi(\phi)$ is a feature that can be defined as $\Phi_W = \Phi_{\max} - \Phi_{\min}$, resulting in

$$\Phi_{\mathrm{W}} = \frac{2\pi dn_{\mathrm{P}}}{\lambda}\left[\left(1-\frac{1}{n_{\mathrm{P}}^2}\right)^{-\frac{1}{2}} - 1\right], \qquad (4)$$

and directly related with experimental data arising from fringe shift counting. Note that the value Φ_{max} corresponds to the case of grazing incidence (*i.e.*, $\phi = \pi/2$), and subsequent refraction within the plate at critical angle $\phi' = \phi'_c$ (see insert in Fig. 1). This situation, however, is not easily to attain in an experiment mainly due to diffraction effects.

3. Experimental set-up

The experimental interferometer can be a Mach-Zehnder interferometer as sketched in the insert of Fig. 2, which is suggested as a very simple way to carry out the proposed experiment [6]. However, the experimental data to be discussed here were obtained from the interferometer of the Fig. 2 for reasons of availability. We used an expanded Argon laser as the coherent light source emitting at $\lambda = 488$ nm, but there is nothing to prevent the use of another coherent light source,

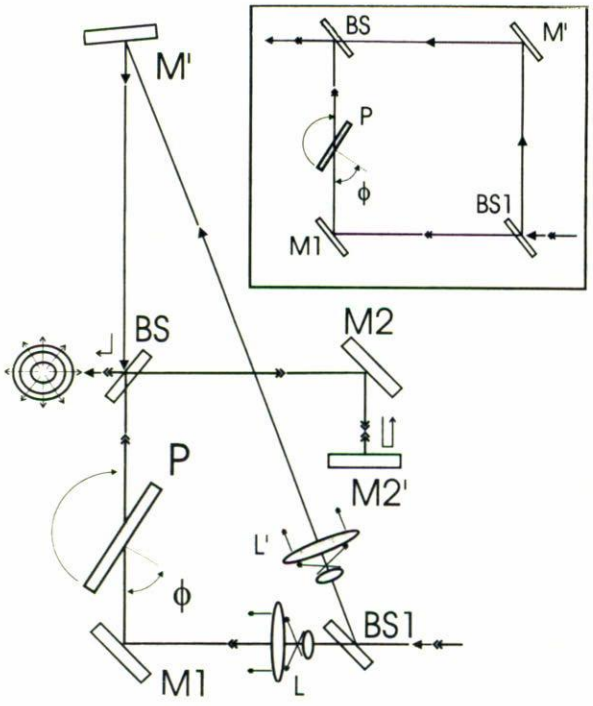

FIGURE 2. Experimental arrangements used for fringe counting. P: transparent parallel plate, M1, M2, M′, M2′: mirrors, L, L′: beam expander/collimating systems, BS1: entrance beam splitter, BS: output beam splitter. Similar notation is employed in the insert.

such as a He-Ne laser source. Light enters the interferometer at BS1, where it is splitted along two paths. One path (object beam) is formed by BS1-M1-BS-M2-M2′-M2-BS. The plate P is placed in this path on a rotatory stage. The second path (reference beam) is BS1-M′-BS. The interferometer is similar to a Mach-Zehnder because the waves interfere one with each other after crossing one-way paths (compare with insert). Collimation of beams were achieved with appropiate optical systems consisting of beam expanders, spatial filters, and collimating lenses (system L and system L′). By slightly defocusing the collimating lens of system L illuminating the plate P, an interference pattern consisting of concentric rings after BS was achieved (rings in front of BS in Fig. 2). Counting of contracting or expanding rings (thus counting of fringe shifts) was carried out taking the center of the pattern as a reference point while tilting a plate (a commercial coverslip) placed on the rotatory stage. Rotation of the plate was done by manipulation of the corresponding knob. Labels on the rotatory stage were found at 2 degrees. Thus, estimation of one degree was needed for the angular reading to be done. In that way, readings of angles ϕ were performed after passing of ten fringes (20π rads) through the reference point. Increasing or decreasing phase differences were taken watching the contraction or expansion of the rings (in front of BS, Fig. 2). Special attention was payed on locating the transition ranges where rings tendency changed from contraction to expansion and viceversa (within 2π accuracy). Other aditional dependance on ϕ was the lateral displacement of the pattern position. This means that it is needed to follow the center of the

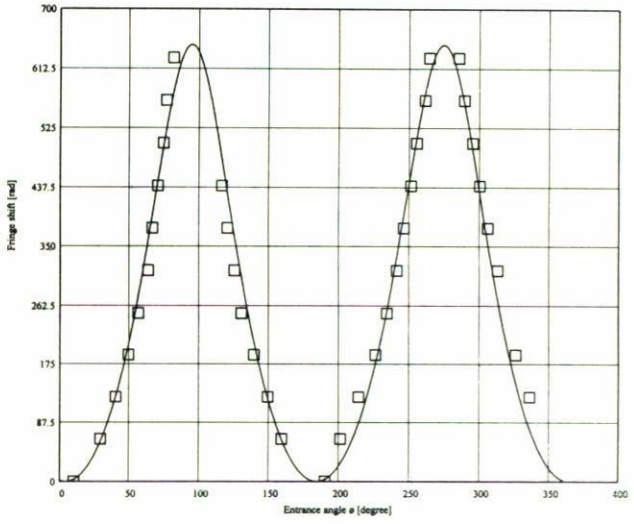

FIGURE 3. Experimental data (squares) obtained with the interferometer of Fig. 2. Preliminary data fitting of $\Delta\Phi(\phi)$ for the data set [Eq. (5)]: assuming $d = 6 \times 10^{-5}$ m, the fitting gives $n_p = 1.248$, $\Phi_{\rm W} = 647.62$ rads, and $\Delta\phi = -4.223°$.

circular pattern along a range while counting fringes. A typical result of fringe shifts (in radians) as a function of the entrance angle ϕ (in degrees) is shown in Fig. 3 (squares). A preliminary fitting to be described in next sections is also shown.

4. Data processing with generalized regression

To verify if the general behaviour of the phase changes obtained by fringe counting as functions of ϕ does follow the prescriptions outlined in Sect. 1, a generalized regression fitting can be performed on the data as presented in Fig. 3. The relative phase changes $\Delta\Phi(\phi) = \Phi(\phi) - \Phi_{\rm min}$ are suitable as fitting functions due to their more direct relation with the data (the value of $\Phi_{\rm min}$ is unknown). Angular errors $\Delta\phi$ of the glass plate from the $0°$ rotatable table mark were taken into account. Here,

$$\Delta\Phi(\phi) = \frac{2\pi d n_{\rm P}}{\lambda}\left\{\left[1 - \left(\frac{\sin(\phi + \Delta\phi)}{n_{\rm P}}\right)^2\right]^{-\frac{1}{2}} - 1\right\}. \quad (5)$$

4.1. Estimation of two parameters and generalized regression

As preliminary fittings of data from Fig. 3, generalized regression fittings with two of the three unknown parameters (d, n_p, and $\Delta\phi$) were performed for estimation. We briefly show the results corresponding to these two cases, denoted by **A** and **B**.

Case A. Data fitting with generalized regression and determination of refractive index

A generalized regression fitting was achieved by using Eq. 5, its first-order partial derivatives with respect to n_p and $\Delta\phi$

and assuming known d. This derivatives permits the use of functions for generalized regression, as the function genfit (**vx**, **vy**, **vg**, **F**) particularly useful for our case [5]. After several attempts looking for a good visual fit, by assuming $d = 6 \times 10^{-5}$ m, we arrive to a fitting giving $n_p = 1.248$, $\Phi_{\rm W} = 647.62$ rads, and $\Delta\phi = -4.223°$. Plot of this fitting is the one to be found in Fig. 3.

Case B. Data fitting with generalized regression and determination of thickness

On the other hand, to check the previous fitting, assuming $n_p = 1.248$, the corresponding fitting by using Eq. (5), its first-order partial derivatives with respect to d, and $\Delta\phi$ [5] delivers $d = 5.98 \times 10^{-5}$ m, $\Phi_{\rm W} = 645.15$ rads, and $\Delta\phi = -4.203°$. These results agrees with the fitting for case A. Another good visual fitting was also found assuming $n_p = 1.212$, giving the following values $d = 5.284 \times 10^{-5}$ m, $\Phi_{\rm W} = 634.8$ rads, and $\Delta\phi = -2.873°$.

We found that the used fitting function [Eq. (5)] does fit the data appropiately. In particular, the values of $\Phi_{\rm W}$ and $\Delta\phi$ are estimated in a very useful way. Both cases render a range width equivalent to about 102 fringes. The values of refractive index and thickness, however, depart very much from the expected ones [7]. This result calls for a further inspection, which, in turn, leads to another fitting approach to be explained in next sections.

4.2. Simultaneous determination of three parameters ($n_p, \Delta\phi, d$) and generalized regression

We first note that different pairs of d and n_p values can deliver the same $\Phi_{\rm W}$ value. In fact, from its definition, it can be shown that a given $\Phi_{\rm W}$ value will render the following d *versus* n_p relationship

$$d = \frac{\lambda \Phi_{\rm W}}{4\pi n_{\rm P}} \left[\left(1 - \frac{1}{n_{\rm p}^2} \right)^{-\frac{1}{2}} - 1 \right]^{-1}, \qquad (6)$$

which plot for $\Phi_{\rm W} = 647$ rads can be found in Fig. 4 as an example. There, the coordinate pair $(1.248, 6 \times 10^{-5})$ found as described in the previous section is approximately just a point on the curve. We note also that the values of $n_p = 1.52$ together with $d = 1.008 \times 10^{-4}$ for example, form another possible pair of values of the same $\Phi_{\rm W}$. But different pairs of values with the same width range $\Phi_{\rm W}$ does not display exactly the same $\Delta\Phi(\phi)$-curve. This can be seen in Fig. 5a for six different pairs of values listed in the table next to the Fig. 5b. To calculate each curve in Fig. 5a, denoted in general by $\Delta\Phi_v(\phi)$, Eq. (5) with $\Delta\phi = 0$ was employed. The smaller the refractive index, the narrower the $\Delta\Phi(\phi)$-curve. In Fig. 5b, the fringe shift differences [determined by $\Delta\Phi_{\rm R}(\phi) - \Delta\Phi_{\rm v}(\phi)$, with $\Delta\Phi_{\rm R}(\phi)$ as a given reference] between a set of values of $\Delta\Phi(\phi)$ with fixed n_p, d pair (the reference $\Delta\Phi_{\rm R}(\phi)$) and a second set with variable n_p, d

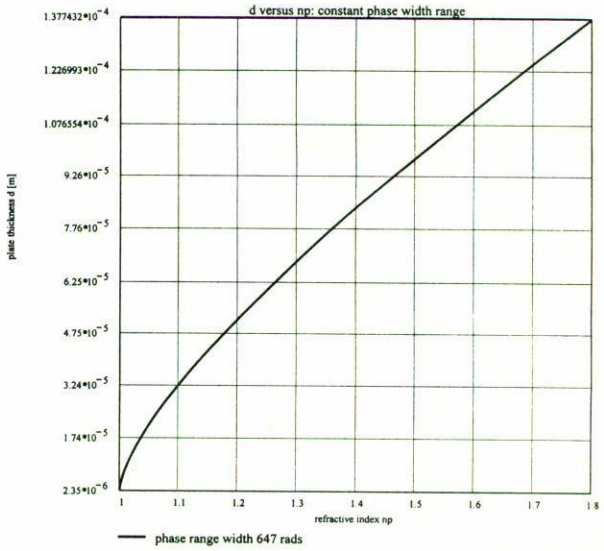

FIGURE 4. Thickness d as a function of the refractive index n_p for the case of a phase width range $\Phi_{\rm W}$ value of 647 rads (solid line). The plot really begins at $n_p = 1.01$.

values, are plotted, at a fixed value of $\Phi_{\rm W}$, for the same six different pair of values n_p and d. As a reference $\Delta\Phi_{\rm R}(\phi)$, the pair $n_p = 1.52$ and $d = 1.008 \times 10^{-4}$ m was taken. Thus, the highest differences correspond to the smallest value of the refractive index. These differences tend to be the highest within a range comprised between 50 and 60 degrees, and another one between 120 and 130 degrees.

These properties open up the possibility of the simultaneous determination of d and n_p as an alternative data processing approach, in which one can rather consider $\Delta\Phi(\phi)$ of Eq. (5) as expressed in terms of $\Phi_{\rm W}$, thus eliminating d by using Eq. (6). This gives

$$\Delta\Phi(\phi) = \Phi_{\rm W} \frac{\sqrt{1 - \dfrac{1}{n_{\rm p}^2}}}{1 - \sqrt{1 - \dfrac{1}{n_{\rm p}^2}}} \times \left\{ \left[1 - \left(\frac{\sin(\phi + \Delta\phi)}{n_{\rm P}} \right)^2 \right]^{-\frac{1}{2}} - 1 \right\}, \qquad (7)$$

that can be used as fitting function instead of Eq. (5). Estimation of $\Phi_{\rm W}$ from data, and fitting of $\Delta\Phi(\phi)$ as given in Eq. (7) using n_p and $\Delta\phi$ as two independent parameters (as well as the first order partial derivatives with respect to n_p and $\Delta\phi$), can lead to the determination of the thickness d over Eq. (6). Assuming $\Phi_{\rm W} = 650$ rads for the data of Fig. 3, this method gives $n_p = 1.529$ and $\Delta\phi = -3.299°$. The calculated value of $\Phi_{\rm W}$ results in 649.844 rads. The corresponding calculation of the thickness through Eq. (6) gives $d = 1.025 \times 10^{-4}$ m. These values of refractive index and thickness correspond to the commercial coverslip refractive index [7] and to direct coverslip's thickness measurement (0.15 ± 0.05 mm) better than the first fittings.

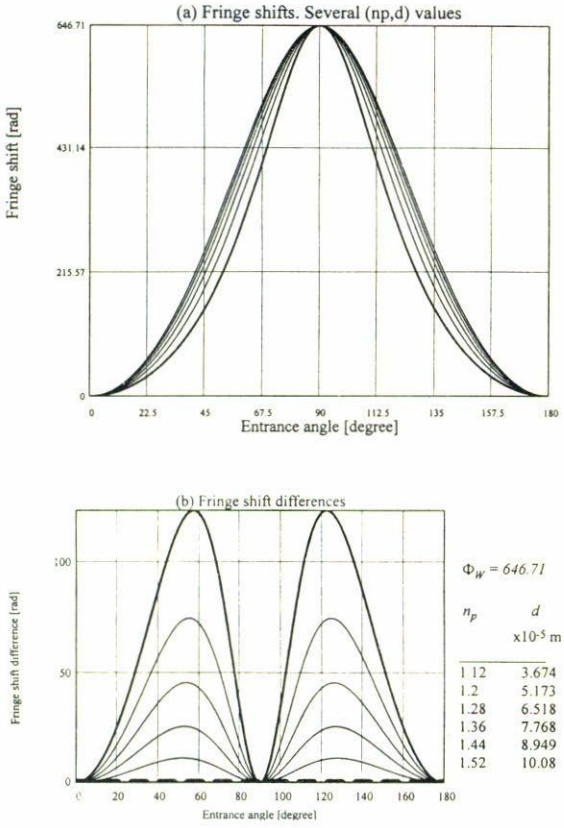

FIGURE 5. a) $\Delta\Phi(\phi)$ for the several values of d and n_p listed in the table below ($\Phi_W = 646.71$). The smaller the refractive index, the narrower the plot of $\Delta\Phi(\phi)$. b) For the same pair of values listed in the table, the fringe shift differences $\Delta\Phi_R(\phi) - \Delta\Phi_v(\phi)$ are plotted as function of ϕ. $\Delta\Phi_R(\phi)$ corresponds to the highest value of the refractive index. The smaller the refractive index, the higher the differences. Each pair of the listed values belongs to a $\Delta\Phi(\phi)$-curve very similar to the one shown in Fig. 4.

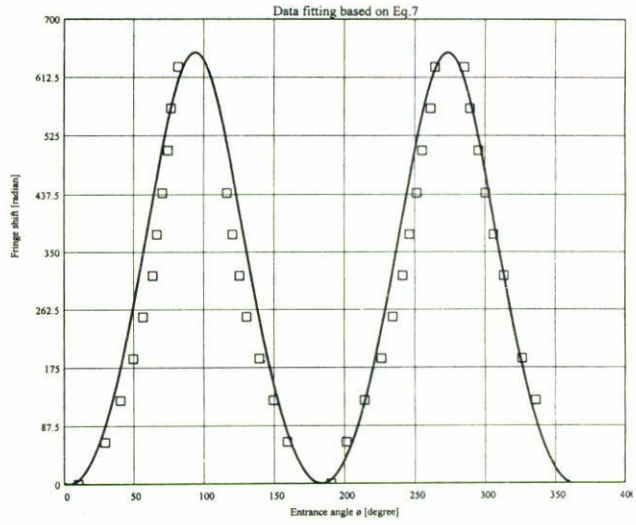

FIGURE 6. Fitting using Eq. 7 and first assuming $\Phi_W = 650$ rads. This gives $\Phi_W = 649.844$ rads, $n_p = 1.529$ and $\Delta\phi = -3.299°$. The calculation of the thickness gives $d = 1.025 \times 10^{-4}$ m, while $\Phi_{max} = 2.667 \times 10^3$ rads and $\Phi_{min} = 2.017 \times 10^3$ rads.

This second fitting method have some features for parameter determination at low precision to be remarked. First, it does not requiere of an independent measurement of one parameter (whether d or n_p). Secondly, it is based on the experimental value of Φ_W, which is a value to be estimated from the same data set. Finally, we have noted more appropiate convergence by employing it. In contrast, while using the first fitting approach, the reaching of a visually good fitting for $\Delta\Phi(\phi)$ was sometimes accomplished only by the use of thickness or refractive index values far away from the expected. This can be seen in the values reported in the Sect. 4.1. An estimation of better precision with the second fitting technique, however, requires of a more precise measurement of Φ_W (fractional order measurement). As a side remark, we note that different pairs of values with the same width range Φ_W will show, in general, different amounts of spherical aberration [compare Eq. (5) with the equivalence criterion between coverslips as discussed in Ref. 7].

A third fitting type, but with the three parameters unknown and independent, gives values of Φ_W again close to the previous ones but with different values of d and n_p as a rule. But the curve at which these resulting n_p, d values belong (according to their Φ_W value, see Fig. 4) contains points (n_p, d) with coordinate values indeed closer to the previous ones. It is possible that by including some minimization constrictions regarding the difference $\Delta\Phi_R(\phi) - \Delta\Phi_v(\phi)$ at the appropiate angular regions, the first and third types of fittings could give more appropiate results.

In addition to the n_p and d parameters, the angular departure $\Delta\phi$ from the normal incidence is also calculated in all fittings. Values of Φ_{max} and Φ_{min} become also available.

5. Final comments

Fringe counting as a measure of the phase changes appearing while tilting a plane parallel plate within an angular range between 0 and 360 degrees behaves in good agreement with the simple model based on the geometrical OPD. This property can be used within the frame of a teaching physics laboratory for illustrative and pedagogical purposes. On the other hand, the technique can derive in a way to inspect parallelism in transparent plane plates based in fringe counting. Some related techniques to inspect plate parallelism are reviewed in Refs. 8 and 9, and others are more recently cited in Ref. 10. Furthermore, fringe counting while tilting plates and an appropiate generalized regression fitting can serve to simultaneously measure both refractive index and thickness at low precision with the aid of an estimation of the experimental phase shift width range Φ_W. We remark that constant angle interference spectroscopy has been proposed to measure refractive index and thickness of transparent layers [4]. The technique uses several wavelengths while holding the tilt angle fixed. In contrast, variable angle monochromatic fringe observation requires two or more wavelengths to determine

both parameters as previously reported [4]. Our proposed technique also measures simultaneously both parameters, but is a technique of a variable angle that needs of only one monochromatic source. The requiring fitting can be found in some software packages widely spread [5]. The experiment can be more easily performed with a Mach-Zehnder interferometer [6] and the corresponding set up requires equipment readily available and usually found on the shelf of most teaching laboratories.

Acknowledgments

Two of the autors (GRZ and JVC) are in leave of absence at Centro de Investigaciones en Optica (CIO) of León, Gto (México) from the Benemérita Universidad Autónoma de Puebla. The authors warmly thank D. Malacara-Hernandez, O. Stavroudis, and R. Rodriguez-Vera for useful discussions. Partial support from CONACyT (codes 3649E and 92984) is also acknowledged.

1. C. Candler, *Modern Interferometers*, (Hilger & Watts Ltd., Glasgow, 1951) Chapt. V, Sect. 5, p. 115.
2. Ealing Corp., "The Measurement of small displacements", in *The User's Manual for the Universal Interferometer* (1979).
3. D. Malacara, "Twyman-Green Interferometer", *Optical Shop Testing*, edited by D. Malacara, (John Wiley and Sons, New York, 1978) Chapt. 2, Sect. 2., p. 58.
4. A.M. Goodman, *Appl. Opt.* **17** (1978) 2779.
5. See Chapt. 13, Statistical functions, Sect. Regression functions, Subsect. Generalized regression, in *Mathcad, User's Guide*, (MathSoft Inc.,1995) p. 309.
6. S. Tolansky, *An Introduction to Interferometry*, (Longmans, Green and Co., London, 1955) Chapt. 9, p. 115.
7. C. Marmasse, *Microscopes and their Uses*, (Science Publications, Gordon and Breach, New York, 1980) Sect. 3.2.9, p. 91.
8. M. Françon, *Optical Interferometry*, (Academic Press, New York, 1966) Sect. 15.1, p. 258.
9. H.D. Bissinger, *Optical Interferograms—Reduction and Interpretation*, edited by Guenther/Liebenberg, symposium sponsored by the American Society for Testing and Materials, (Phyladelphia, 1978) p. 11.
10. A. Jaramillo-Nuñez, C. Robledo-Sanchez, and A. Cornejo-Rodriguez, *Opt. Eng.* **35** (1996) 3437.